



HAL
open science

Enhancing uranium extraction efficiency using protonated amines and quaternary ammonium-based ionic liquids: mechanistic insights and nonlinearities analysis

Elise Guerinoni, Sandrine Dourdain, Thomas Dumas, Guilhem Arrachart, Fabrice Giusti, Zijun Lu, Pier-Lorenzo Solari, Stéphane Pellet-Rostaing

► To cite this version:

Elise Guerinoni, Sandrine Dourdain, Thomas Dumas, Guilhem Arrachart, Fabrice Giusti, et al.. Enhancing uranium extraction efficiency using protonated amines and quaternary ammonium-based ionic liquids: mechanistic insights and nonlinearities analysis. *Separations*, 2023, 10, pp.509. 10.3390/separations10090509 . hal-04224208

HAL Id: hal-04224208

<https://hal.science/hal-04224208v1>

Submitted on 13 Nov 2023

HAL is a multi-disciplinary open access archive for the deposit and dissemination of scientific research documents, whether they are published or not. The documents may come from teaching and research institutions in France or abroad, or from public or private research centers.



L'archive ouverte pluridisciplinaire **HAL**, est destinée au dépôt et à la diffusion de documents scientifiques de niveau recherche, publiés ou non, émanant des établissements d'enseignement et de recherche français ou étrangers, des laboratoires publics ou privés.



Distributed under a Creative Commons Attribution 4.0 International License

Article

Enhancing Uranium Extraction Efficiency Using Protonated Amines and Quaternary Ammoniums-Based Ionic Liquids: Mechanistic Insights and Nonlinearities Analysis

Elise Guerinoni ¹, Sandrine Dourdain ^{1,*}, Thomas Dumas ², Guilhem Arrachart ¹ , Fabrice Giusti ¹ , Zijun Lu ¹, Pier-Lorenzo Solari ³ and Stéphane Pellet-Rostaing ¹ 

¹ ICSM, CEA, Univ Montpellier, CNRS, ENSCM, 30207 Marcoule, France; elise.guerinoni@cea.fr (E.G.); guilhem.arrachart@cea.fr (G.A.); fabrice.giusti@cea.fr (F.G.); zijun.lu@cea.fr (Z.L.); stephane.pellet-rostaing@cea.fr (S.P.-R.)

² CEA, DES, ISEC, DMRC, Univ Montpellier, 30207 Marcoule, France; thomas.dumas@cea.fr

³ Synchrotron SOLEIL, MARS Beamline, BP 48, 91192 Gif Sur Yvette, France; pier-lorenzo.solari@synchrotron-soleil.fr

* Correspondence: sandrine.dourdain@cea.fr

Abstract: This study investigates uranium solvent extraction under AMEX process conditions. The use of pure extractants without diluents or phase modifiers allows us not only to reduce the use of volatile organic compounds but also to provide higher extraction yields without third-phase formation. Pure extractants are protonated amines or quaternary ammoniums with suitable counter ions, which act at the interface between ion pairs and protic ionic liquids. The mixture of sulphates anion (SO_4^{2-}) and bis(trifluoromethanesulfonyl)imide anion (NTf_2^-) revealed unexpected nonlinear extraction behaviors, which appear highly important to rationalize for optimized application. A spectroscopic analysis (NMR, UV-vis, FT-IR, and EXAFS) showed that uranium extraction occurs via a protonated amine and three sulphates. A nonlinear extraction could further be interpreted by considering a water and acid transfer between the two phases: at lower sulphate ratios, the release of acid from the organic phase into the aqueous phase was shown to influence the number of protonated amines in the organic phase, affecting uranium extraction before its enhancement. Furthermore, the extraction loss at higher sulphate ratios was assigned to the destabilization of bidentate uranium–sulphate complexes due to a competition between water and sulphates.

Keywords: solvent extraction; ionic liquids; mechanism; spectroscopy; anion mixture; nonlinearity



Citation: Guerinoni, E.; Dourdain, S.; Dumas, T.; Arrachart, G.; Giusti, F.; Lu, Z.; Solari, P.-L.; Pellet-Rostaing, S. Enhancing Uranium Extraction Efficiency Using Protonated Amines and Quaternary Ammoniums-Based Ionic Liquids: Mechanistic Insights and Nonlinearities Analysis.

Separations **2023**, *10*, 509. <https://doi.org/10.3390/separations10090509>

Academic Editor: Sascha Nowak

Received: 28 July 2023

Revised: 6 September 2023

Accepted: 12 September 2023

Published: 15 September 2023



Copyright: © 2023 by the authors. Licensee MDPI, Basel, Switzerland. This article is an open access article distributed under the terms and conditions of the Creative Commons Attribution (CC BY) license (<https://creativecommons.org/licenses/by/4.0/>).

1. Introduction

In the context of the recent energy crisis, nuclear power is an established technology that has been chosen by several countries to provide low-carbon electricity. It requires, however, a huge amount of uranium, whose extraction from mines relies on hydrometallurgical processes. The amine extraction (AMEX) process is based on mixtures of alkyl amines in aliphatic diluent with fatty alcohol [1]. Despite its extensive application for uranium purification in the front end of the nuclear fuel cycle, this process faces several problems, including non-ideal uranium separation, the requirement of a phase modifier (fatty alcohol) to prevent third-phase formation, and possible extractant degradation due to the presence of vanadium and a phase modifier [2–4].

In particular, the Somair uranium extraction and purification plant in Niger has a stock of around 900 m³ of solvent, 75% of which is replaced each year due to formulation degradation (crud formation), loss through the entrainment of the organic phase in the aqueous phase, or evaporation.

Numerous alternatives are currently being studied to avoid the use of volatile organic compounds for metal separation. For example, solid–liquid extraction [5], supercritical

extraction [6], and flotation [7] have been proposed. However, they remain difficult to apply to uranium extraction, as they require a complete rethink of the industrial process and facilities. Interesting alternatives also include the simple replacement of organic solvents with non-volatile solvents such as ionic liquids (ILs) or deep eutectic solvents [8,9].

Under AMEX process conditions [1,10], it has been demonstrated and patented that the use of pure extractants (trialkylamines), without diluent and phase modifiers enables higher extraction yields without third-phase formation [11,12]. Pure extractants are quaternary ammoniums or trialkylamines previously protonated and associated with a counteranion. These pure amines and quaternary ammoniums actually lie at the interface between the amine (ion pair) and protic ionic liquid (quaternary ammonium) chemistry and have already been used as ionic liquids for liquid–liquid extraction [13–15]. Such ionic liquids are often used as diluents to increase the extraction capacity of a ligand, but they are more than a plain diluent. They modify the extraction mechanism through the participation of their anion or cation in the metal complex or by inducing a different organization of the organic phase [16–18]. Many studies have been dedicated to the mechanisms of solvent extraction in ILs. Billard et al. [19] proposed two equilibria (cationic and anionic exchanges) to summarize the possible ion exchange mechanisms when ILs are used as diluents. It was found out that ion exchange is the dominant mechanism for uranium and actinides extraction.

A wide range of ILs have also been used as extractants in aliphatic diluents, to which phase modifiers are sometimes added [20–23]. Depending on the anions and cations they contain, ILs can be highly hydrophobic and present a sufficiently low viscosity at room temperature to be used both as an extraction agent and as a hydrophobic phase. In this case, dilution in an aliphatic diluent is not necessary. Extraction performance and selectivity is usually improved compared to conventional solvents [24–27].

Mixtures of ILs may also be applied, as they generally combine the properties of two different ILs. For instance, a “diluting” IL with advantageous transport properties (low viscosity and high conductivity), can be mixed with a “complexing” IL whose transport properties are prohibitive for use at low temperatures [28,29].

In the present study, diluent-free quaternary ammoniums or trialkylamines and their mixtures were assessed under the conditions of the AMEX process. The topological formula of the involved anion and cation is given in Figure 1, where TOAH⁺ stands for trioctylammonium, MTOA⁺ for methyltrioctylammonium, and the commercial Aliquat 336⁺ is composed of a mixture of MTOA⁺ and methyltridecylammonium (MTDA⁺). Sulphate (SO₄²⁻), chloride (Cl⁻), and bis(trifluoromethanesulfonyl)imide (NTf₂⁻) were chosen to evaluate the anion effect on uranium extraction.

The various tested mixtures provided high extraction efficiency with nonlinear properties. A mechanistic study is proposed to elucidate the uranyl extraction mechanisms of the [TOAH]₂[SO₄] + [TOAH][NTf₂] mixture. As it might be very interesting to design mixtures with optimized extraction properties, the origin of these nonlinearities is investigated in detail in this study. The coordination of uranyl was evaluated via NMR, UV-vis, and EXAFS spectroscopy. Considering the water and acid transfer between the two phase, FT-IR spectroscopy was further used to elucidate the various regimes of the extraction of this mixture.

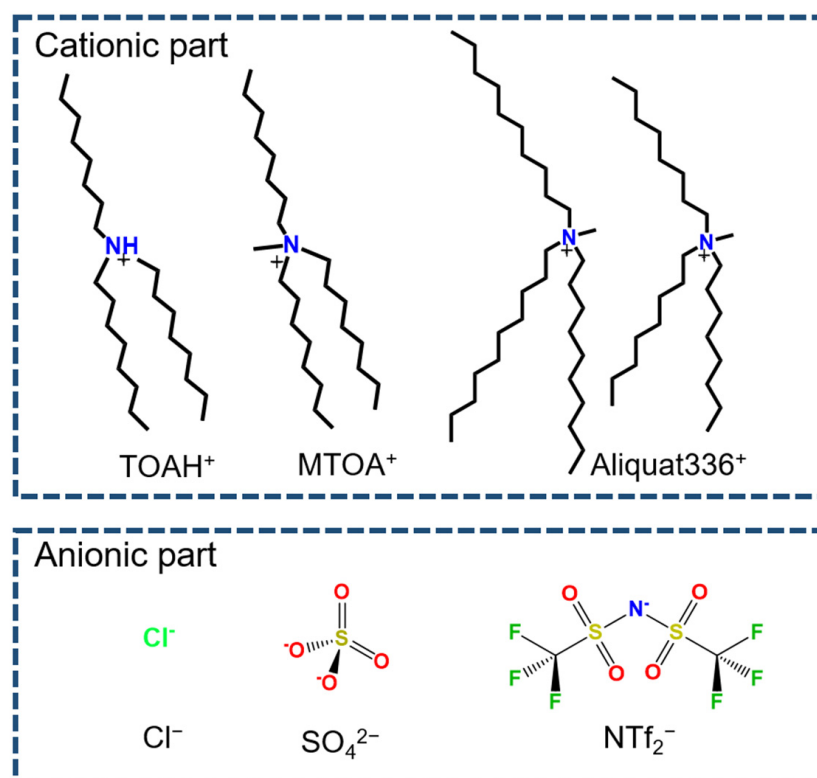


Figure 1. Structure of cations investigated (**top**): trioctylammonium ([TOAH]⁺), methyltrioctylammonium ([MTOA]⁺) and Aliquat 336. Structure of anions tested (**bottom**): sulphate (SO₄²⁻), chloride (Cl⁻) and bis(trifluoromethanesulfonyl)imide (NTf₂⁻).

2. Materials and Methods

2.1. Chemicals and Reagents

Trioctylamine (TOA) 98%, sulphuric acid 96%, and ammonium sulphate were purchased from Sigma-Aldrich (Saint Quentin Fallavier, France). Aliquat 336 and lithium bis(trifluoromethanesulfonyl)imide (LiNTf₂) were supplied by Alfa Aesar (Thermo Fisher Scientific, Geel–Belgium) and ABCR (Karlsruhe, Germany), respectively. Methyltrioctylammonium chloride ([MTOA][Cl]) and methyltrioctylammonium bis(trifluoromethanesulfonyl)imide ([MTOA][NTf₂]) were purchased from ABCR. All chemicals were used as received, without any further purification.

2.2. Instrumentation and Analysis

Metal concentration was determined by inductively coupled plasma optical emission spectroscopy (ICP-OES Spectro Arcos—AMETEK Materials Analysis, Kleve, Germany or ThermoFisher Scientific, Courtaboeuf, France). Prior to concentration measurements, aliquots of uranium and iron stock and working solutions were diluted with a v:v 0.99% nitric acid solution in order to bring the concentration into the 1–15 mg.L⁻¹ range. Metal quantification was performed at several wavelengths. Uranium was detected at 393.203 nm, 385.466 nm, and 385.958 nm; iron was detected at 239.562 nm, 240.488 nm, and 259.940 nm. Calibration samples were prepared from 1000 mg.L⁻¹ uranium and iron standards (SCP Science PlasmaCal). Uncertainties in metal concentrations were determined statistically by repeated measurements.

The amount of extracted acid was determined via acid–base titration using a Metrohm 905 titrando automatic potentiometer. A sample of aqueous phase was taken and dosed with a 0.01 mol.L⁻¹ NaOH solution. The concentration of sulfuric acid in the organic phases was given by subtracting the acidity of the aqueous phase measured at equilibrium from that of the initial aqueous phase. The amount of water present in the organic phases was determined using the Karl Fischer method with a Metrohm coulometer.

The speciation of uranium complexes in ionic liquid media was achieved via ultra violet–visible and Fourier transform infrared spectroscopies (UV-vis and FT-IR). UV-vis spectra were recorded between 200 and 800 nm on a dual-beam Varian Cary 5000 spectrophotometer in plastic cells with a 2 mm optical path. The absorbances of contacted, pre-contacted, and non-contacted samples were measured using an empty cell in the second beam as a reference. Subtractions were calculated post-processing. At a given wavelength, λ , the absorbance, A , of a mixture of n absorbing species is the sum of the individual absorbances. The signal from the species formed by water and acid can therefore be subtracted to highlight uranium-related signals. Infrared spectra of ionic liquid phases were recorded on a Bruker Vertex 70 FT-IR spectrometer equipped with a diamond ATR. A blank was run on air before each measurement. The Fourier transform was calculated using Perkin Elmer's Spectrum software, then the background noise was subtracted. The measurement range extends from 4000 to 615 cm^{-1} . Many absorption bands were found in the printed part of the spectrum of interest in this study. The pre-contacted sample signal was subtracted to highlight the uranium-related absorption bands. A Voigt function was used to best fit the signal and calculate the area under the curves of the highlighted spectra.

X-ray absorption spectroscopy (Extended X-ray Absorption Fine Structure-EXAFS) was carried out on the MARS (Multi-Analyses on Radioactive Samples) light line at the SOLEIL synchrotron (Saint-Aubin, France) (proposal ID: 20210696). Spectra were recorded at the uranium LIII threshold (17,167 eV). Calibrations were carried out at the yttrium K threshold (17,039 eV).

In practice, samples were placed in double-confinement EXAFS cells, enabling active samples to be measured. The cells can hold a maximum of 12 samples. The volume of each sample was 0.25 mL.

Data were processed using the Athena program. EXAFS oscillations are extracted in several steps. The ionization energy threshold, E_0 , is defined by taking the maximum of the derivative at the threshold jump. After signal normalization using linear and cubic functions, the signal can be converted from E (eV) energy space to k (\AA^{-1}) wavenumber space. To increase the amplitude of oscillations observed at high wavenumbers, a k^2 or k^3 factor can be applied. Once the oscillations have been extracted, a conversion to real distance space, R (\AA), is performed by applying a Fourier transform to the EXAFS k^3 signal, $\chi(k)$, over a defined wavenumber range (in the remainder of this study, this range is $3.75 < k < 14$). Finally, the pseudo-radial distribution function is obtained as a function of R . This pseudo-radial distribution function schematically represents the probability of atoms being present around the absorber atom as a function of their distance increased by a phase shift φ . It is not the actual distance, R , from the absorber atom. Fits were then made in the Artemis software. The uranyl trisulphate scattering paths and amplitudes were calculated using FEFF 8.4 from a selected structure issued from the same molecular dynamic model as in Sukbaataar et al. [30]. The discrepancy between the fitted data and the experimentally found data can be expressed by calculating the R factor based on the method of least squares.

Fluorine-19 nuclear magnetic resonance spectroscopy (^{19}F -NMR) was also used to study the impact of metal extraction on the chemical shift of the fluorine function of NTf_2 . Double-walled tubes were used so as not to alter the chemistry of the organic phase and so that a reference solvent (deuterated DMSO) could be applied externally.

2.3. Extraction Experiments

Several organic extractants based on protonated tertiary amines or quaternary ammoniums and their mixtures were evaluated in this work for the extraction of uranium in sulfuric media. Their synthesis is described in ESI 1.

Organic phases were prepared by mixing protonated tertiary amines or quaternary ammoniums (defined as Am 1 and Am 2) in different proportions. Samples were classified according to their molar ratio of Am 1, $x_{Am\ 1}$, defined as follows:

$$x_{Am\ 1} = \frac{n(Am\ 1)}{n(Am\ 1) + n(Am\ 2)}$$

The aqueous phases used in this study were prepared by dissolving the uranium sulphate, $UO_2SO_4 \cdot 6.38H_2O$, M.W. = 479.43 $g \cdot mol^{-1}$, and the iron sulphate, $Fe_2(SO_4)_3 \cdot 8.3H_2O$, M.W. = 549.46 $g \cdot mol^{-1}$.

The acidity of the solution was controlled by adding sulfuric acid (v:v H_2SO_4 96%, M.W. = 98.08 $g \cdot mol^{-1}$), and the sulphate concentration was increased by adding ammonium sulphate ($(NH_4)_2SO_4$, M = 132.14 $g \cdot mol^{-1}$).

The aqueous and organic phases are brought into contact in Eppendorf tubes of an appropriate volume and stirred (500 rpm) for 1 h at 20 °C in a thermostatically controlled cell (Infor-ht[®] ecotron). The phases are then separated after a centrifugation step (Rotina 380R) lasting between 5 and 20 min at a rotation speed of 8000 rpm. The phases are then separated in 2 different flasks before sampling for analysis.

$$D_M = \frac{\sum a_{M,org,eq}}{\sum a_{M,aq,eq}}$$

where $\sum a_{M,org,eq}$ stands for the sum of the chemical activities of a solute M in all its forms in the organic phase and $\sum a_{M,aq,eq}$ for the sum of the chemical activities of the same solute in all its forms in the aqueous phase. In dilute media, activity is equal to molar concentration.

3. Results and Discussion

Several commercial quaternary ammonium ligands and their mixtures were evaluated for uranium extraction from sulphuric media. Their performances were compared with the classical trioctylamine extractant (taken as reference for the AMEX process) solubilised in dodecane in the presence of 1-octanol as a phase modifier. The evaluated cations and anions are illustrated in Figure 1. The distribution ratios of the uranium obtained with these ammoniums salts and mixtures are displayed in Figure 2.

The results show that uranium extraction is not only driven by the nature of cations and anions but also by the ratio between them. When similar cations are considered, systems with SO_4^{2-} extract better than with Cl^- (see Figure 2b). Whatever the cation, no extraction occurred when NTf_2^- was used as anion (see left side of Figure 2a–d and green line in Figure 2d). Uranium extraction increases with sulphate concentrations, which is consistent with the recognized extraction mechanisms for such systems; as demonstrated by Sukhbaatar et al. [30], uranium extraction from sulphuric media requires the formation of uranyl trisulphate complexes.

Looking at the effect of the cations, Figure 2 shows, moreover, that $TOAH^+$ extracts more uranium than $MTOA^+$ and than Aliquat 336 when the counter anion is a sulphate (right side of Figure 2a–c).

Interestingly, uranium extraction is not linear with the molar ratio of one quaternary ammonium to another but shows nonlinearities with a synergistic peak when mixtures of anions are involved (see Table 1 for position of the synergistic peaks).

Overall, nonlinear extraction is observed when the cations are identical and when the anion is modified. In contrast, when the anion is identical and the cation is modified, linear extraction is obtained. We can therefore conclude that the nonlinearities observed are due to anion mixing and not cation mixing.

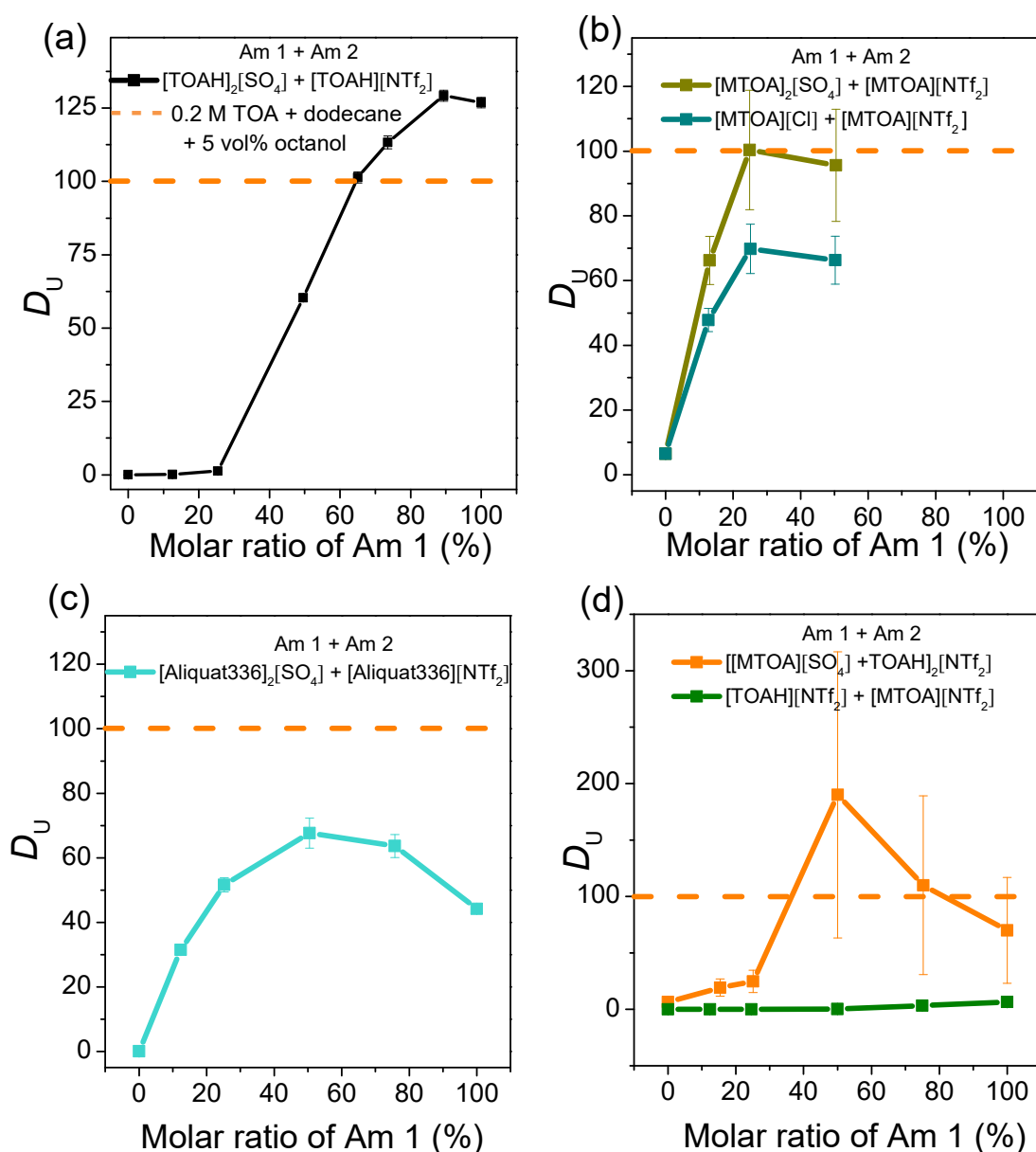


Figure 2. (a) Distribution coefficients of U of quaternary ammoniums mixtures carrying same cation and different anions (a–c) or different cations (d). Initial aqueous solution contains 0.1 mol.L⁻¹ sulfuric acid (pH = 1), 1 mol.L⁻¹ ammonium sulphate, 2500 mg.L⁻¹ U(VI), and 250 mg.L⁻¹ Fe (III) for (a) and 0.1 mol.L⁻¹ sulfuric acid (pH = 1), 0.1 mol.L⁻¹ ammonium sulphate, 250 mg.L⁻¹ U(VI), and 250 mg.L⁻¹ Fe (III) for (b–d). A/O = 2. Distribution coefficients of U measured in the same conditions for the reference system TOA-dodecane are presented in dashed orange lines on all graphs. Composition of Aliquat 336 is given in Supplementary Materials. Molar ratios higher than 50% are not presented in Figure 2b because the mixtures were not liquid/soluble.

Table 1. Synergistic peak position and distribution coefficient of uranium (data extracted from Figure 2).

	[MTOA] ₂ [SO ₄] + [MTOA][NTf ₂]	[MTOA][Cl] + [MTOA][NTf ₂]	[Aliquat336] ₂ [SO ₄] + [Aliquat336][NTf ₂]	[MTOA][NTf ₂] + [TOAH] ₂ [SO ₄]	[TOAH] ₂ [SO ₄] + [TOAH][NTf ₂]
Ratio (%)	25	25	50	50	90
D_U	100	70	78	196	128

Depending on the system, such a synergic mixture may provide higher extraction than the pure component. While a small difference is observed between the 90% $[\text{TOAH}]_2[\text{SO}_4]$ and 10% $[\text{TOAH}][\text{NTf}_2]$ mixture, a significant increase in extraction is obtained for the system $[\text{Aliquat336}]_2[\text{SO}_4] + [\text{Aliquat336}][\text{NTf}_2]$. It is also interesting to consider that such mixtures may also be interesting for other properties than uranium extraction, such as viscosity or density [31]. As it might be very promising to design mixtures with optimized extraction properties, the origins of these nonlinearities have been investigated in more details for the mixture $[\text{TOAH}]_2[\text{SO}_4]$ and $[\text{TOAH}][\text{NTf}_2]$. This peculiar system is interesting not only because it is the most efficient one toward uranium extraction but also because its extraction nonlinearities show three distinct regimes (Figure 2a): extraction is initially antagonistic (lower than the linear mixture), then synergistically increased, and finally decreased for the higher sulphate ratios. The extraction mechanisms of the $[\text{TOAH}]_2[\text{SO}_4] + [\text{TOAH}]_2[\text{NTf}_2]$ mixture were therefore investigated with a spectroscopic study combined with a detailed analysis of the sulphate effect on the uranium, acid, and water transfer between the organic and aqueous phases.

3.1. Effect of the Amount of Sulphates in the Aqueous Phase

Like sulphates in the organic phase, the amount of sulphates in the aqueous phase may affect uranium extraction. In order to evaluate this effect, the sulphate concentration in the aqueous phase was varied by changing the concentration of ammonium sulphate. The effects on uranium extraction and acid and water transfer are presented in Figure 3 for sulphate concentrations of $[(\text{NH}_4)_2\text{SO}_4] = 0.1$ and 1 mol.L^{-1} in the aqueous phase.

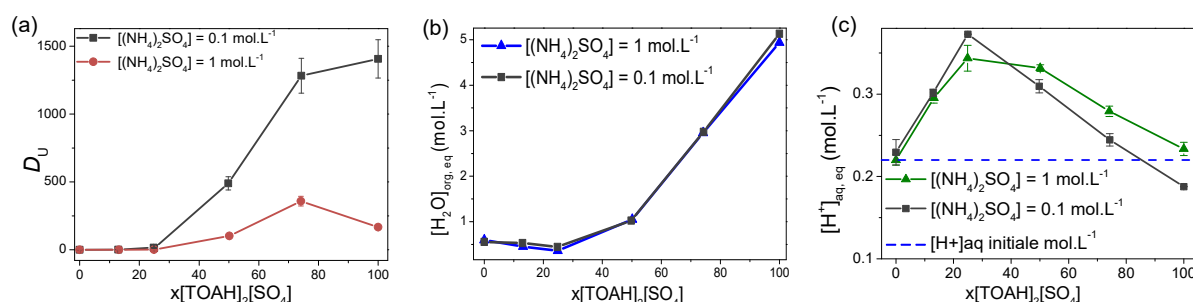


Figure 3. (a) Uranium distribution coefficient, (b) concentration of water in the organic phase after contact, and (c) concentration of acid in the aqueous phase after contact, measured for each mixture $[\text{TOAH}]_2[\text{SO}_4] + [\text{TOAH}][\text{NTf}_2]$ for 2 concentrations $[(\text{NH}_4)_2\text{SO}_4] = 0.1$ and 1 mol.L^{-1} in the aqueous phase. A/O = 2. Composition of aqueous phase: $250 \text{ mg.L}^{-1} \text{ U(VI)}$, $250 \text{ mg.L}^{-1} \text{ Fe(III)}$, $0.1 \text{ mol.L}^{-1} \text{ H}_2\text{SO}_4$.

Figure 3a shows that increasing the sulphate concentration in the aqueous phase decreases uranium extraction for all $x[\text{TOAH}]_2[\text{SO}_4]$ ratios. It is also interesting to note that the decrease in D_U between 75 and 100% sulphate is most marked for $[(\text{NH}_4)_2\text{SO}_4] = 1 \text{ mol.L}^{-1}$. The water concentration (Figure 3b) is unaffected by the amount of ammonium sulphate, while the acid transfer between the two phases is a little affected (Figure 3c). Water content is also not affected by the presence of acid or uranium in the aqueous phase (Figure S1). The acid transfer is actually unexpected. Instead of being extracted in the organic phase with the metal (as is usually the case in solvent extraction), acid is released from the organic toward the aqueous phase. This acid release is attributed to the deprotonation of the TOAH^+ originally present in the organic phase. It appears to be poorly affected by the $(\text{NH}_4)_2\text{SO}_4$ concentration for the low $x[\text{TOAH}]_2[\text{SO}_4]$ ratios, while it is slightly increased above $x[\text{TOAH}]_2[\text{SO}_4] = 50\%$.

This experiment shows, therefore, that uranium extraction is both dependent on the amount of sulphate present in the aqueous and in the organic phase. Most importantly, it also shows that the decrease in uranium extraction at high $x[\text{TOAH}]_2[\text{SO}_4]$ ratios is concomitant with an increase in the release of H^+ protons in the aqueous phase (expected

to decrease the concentration of protonated TOA in the organic phase), as well as with a strong increase in water extraction in the organic phase.

To further understand the nonlinear relationship between uranium extraction and the $x[\text{TOAH}]_2[\text{SO}_4]$ ratios, the remainder of this paper is devoted to characterizing the uranyl complexes extracted in the organic phase. It is indeed important to evaluate if uranium is chelated as in the conventional medium (TOA in dodecane) or if the NTf_2^- anion is involved to form mixed complexes for some $x[\text{TOAH}]_2[\text{SO}_4]$ ratios.

3.2. Characterizing the Extracted Species

3.2.1. NTf_2^- Participation in the Uranium Complex

To obtain information about the chemical environment of NTf_2^- in the binary mixtures before and after uranium extraction, ^{19}F -NMR and FT-IR measurements were carried out. Note that NTf_2^- gives only one resonance band in the ^{19}F -NMR spectra. Its evolution provides information on the environmental change in the NTf_2^- . ^{19}F -NMR spectra of the $[\text{TOAH}]_2[\text{SO}_4] + [\text{TOAH}][\text{NTf}_2]$ mixtures, which are plotted in Figure 4a for $x[\text{TOAH}]_2[\text{SO}_4] = 50\%$. It shows that the chemical shift for NTf_2^- is not modified before and after uranium extraction, which indicates that NTf_2^- does not directly coordinate uranyl.

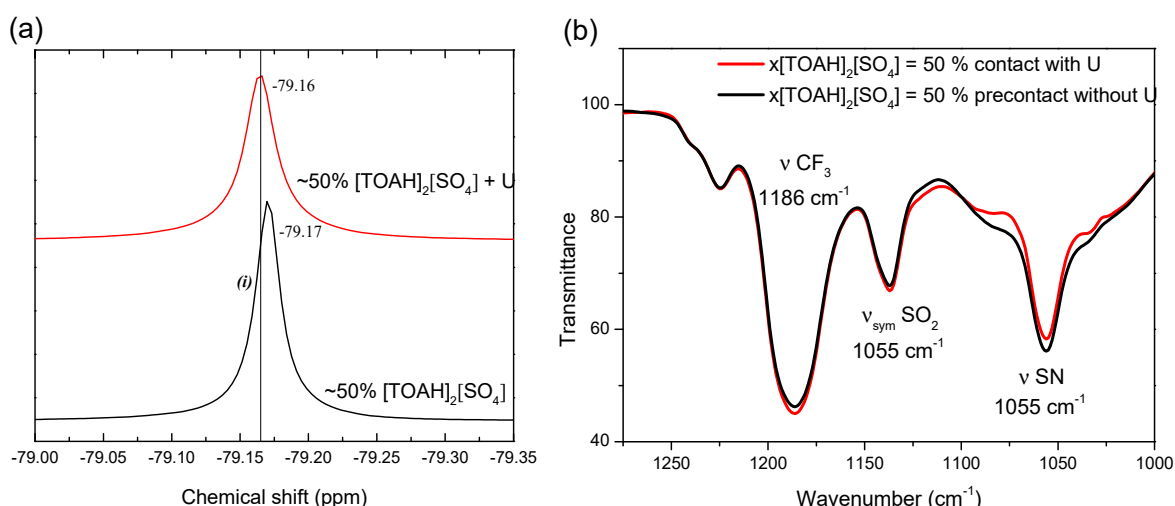


Figure 4. (a) ^{19}F -NMR spectrum and (b) FT-IR spectra of the mixture $x[\text{TOAH}]_2[\text{SO}_4] = 50\%$. Black is before and red is after contact with an aqueous phase containing $2500 \text{ mg}\cdot\text{L}^{-1}$ U(VI), $0.1 \text{ mol}\cdot\text{L}^{-1}$ sulfuric acid, and $1 \text{ mol}\cdot\text{L}^{-1}$ ammonium sulphates. A/O = 4.

This conclusion is reinforced by the Fourier transform infra-red (FT-IR) analysis shown in Figure 4b. It can be observed that the characteristic bands of NTf_2^- [32] are not affected by the presence of uranium. NTf_2^- therefore does not participate directly in the complex with uranium, and the extraction nonlinearities of the mixture cannot be explained by the formation of a synergistic or antagonistic mixed complex of uranium with sulphates and NTf_2^- .

3.2.2. UV-Vis Spectroscopy and EXAFS, Study of First Neighbors

To determine whether the origin of the nonlinear extraction is due to uranium speciation, UV-vis uranium spectroscopy and X-ray absorption spectroscopy (EXAFS) measurements were performed for various $x[\text{TOAH}]_2[\text{SO}_4]$ ratios.

The UV-vis spectra recorded after contact with a uranium solution (Figure 5a) show the same type of fingerprint signal for 25 to 100% ratios as for the conventional medium (TOA + dodecane + octanol) shown in the dotted orange line. The different trend observed for the ratio 0% is due to the absence of uranium in this sample. As demonstrated by Servaes et al. who studied the speciation of uranyl nitrate complexes in acetonitrile and ionic liquid [33], this fingerprint is characteristic of a trigonal symmetric uranium complex.

In their study, the spectra of $[\text{UO}_2(\text{NO}_3)_3]^-$ complexes in acetonitrile or in $[\text{C}_4\text{mim}][\text{NTf}_2]$ show signals similar to those observed for $[\text{UO}_2(\text{CO}_3)_3]^{4-}$ and $[\text{UO}_2(\text{CH}_3\text{COO})_3]^-$ complexes [34]. By comparing the experimental spectra with those reported in the literature, it can therefore be concluded that for all $x[\text{TOAH}]_2[\text{SO}_4]$ ratios, the uranyl–sulphate complex exhibits D_{3h} trigonal symmetry, suggesting that uranyl is complexed with three sulphates in an ionic liquid medium. EXAFS spectroscopy measurements were carried out to confirm this hypothesis.

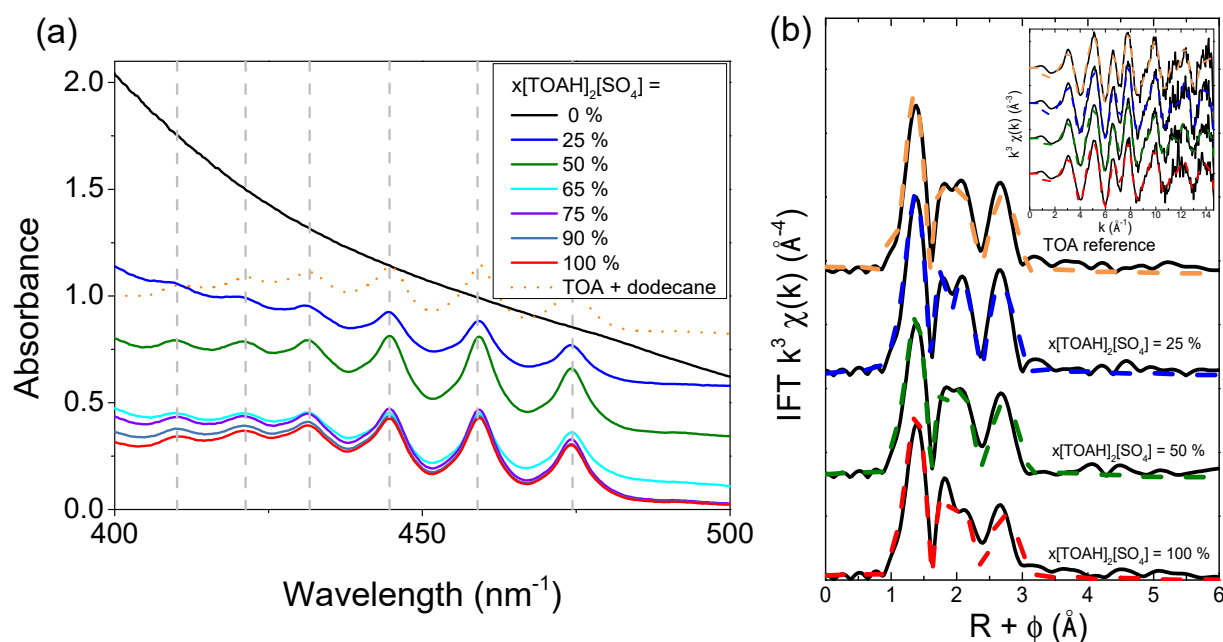


Figure 5. (a) Raw UV-vis data for uranyl in the mixtures $[\text{TOAH}]_2[\text{SO}_4] + [\text{TOAH}][\text{NTf}_2]$ ($x[\text{TOAH}]_2[\text{SO}_4] = 25$ to 100%) and in the reference medium TOA + dodecane. (b) Experimental (solid lines) and fitted (dotted lines) EXAFS spectra: k^3 -weighted Fourier transforms of the 3-sulphate bidentate model around uranyl. The orange line represents the reference system; the blue, green, and red lines represent the compositions $x[\text{TOAH}]_2[\text{SO}_4] = 25, 50,$ and 100% , respectively. (b) Structure of uranium sulphate; the different contributions to the EXAFS spectra are indicated by red dotted lines.

Figure 5b displays the EXAFS spectra measured at the L3 threshold of uranium and the corresponding Fourier transforms. No EXAFS spectra could be measured for $x[\text{TOAH}]_2[\text{SO}_4]$ ratios lower than 25% , as the uranium concentrations were too small in these samples. For higher $x[\text{TOAH}]_2[\text{SO}_4]$ ratios, it is apparent that the experimental spectra (solid lines) obtained with the $[\text{TOAH}]_2[\text{SO}_4] + [\text{TOAH}][\text{NTf}_2]$ mixtures are very similar to the ones measured in conventional media (orange spectrum, TOA + dodecane). It can also be noted that, in addition to the first $\text{U}-\text{O}_{yl}$ contribution of linear transdioxo bonds ($R + \phi = 1.2 \text{ \AA}$) and that of the equatorial $\text{U}-\text{O}_{eq}$ oxygen coordination layer ($R + \phi = 1.8$ to 2.4 \AA), the spectra show intense contributions in the second coordination sphere ($R + \phi > 2.5 \text{ \AA}$) due to sulfur atoms of sulphate anions coordinated with UO_2^{2+} [30,35].

In a previous study carried out in a conventional medium (TOA + dodecane), coupling a classical fit with molecular dynamics simulations enabled the unravelling of the speciation of uranium in the organic phase; the complex consisted of three sulphate anions coordinated to uranyl via U-O bonds in the first coordination sphere [30]. The study also showed that uranyl trisulphate complexes shift from a configuration with three bidentate sulphates to a configuration with two bidentate and one monodentate. The most favorable configuration is still the tri bidentate sulphate configuration.

In order to probe more precisely the local structure of uranyl in [TOAH]₂[SO₄] + [TOAH][NTf₂] mixtures, a fit of the EXAFS spectra was performed by applying a structural model of three bidentate sulphates in the first uranium sphere. The fitted parameters are presented in Table 2, and the corresponding fitted spectra are plotted as dotted lines in Figure 5b.

Table 2. Parameters of the best fit obtained for EXAFS spectra of [UO₂(SO₄)₃]^{4−} complexes. (σ^2 is the Debye–Waller factor accounting for disorder, ΔE_0 is the energy fit, S_0^2 is the amplitude factor, and R -factor is the tuning factor). ^a fixed parameters.

	x[TOAH] ₂ [SO ₄] = 25%			x[TOAH] ₂ [SO ₄] = 50%			x[TOAH] ₂ [SO ₄] = 100%			TOA + Dodecane			
	<i>N</i>	<i>R</i> (Å)	σ^2 (Å ²)	<i>N</i>	<i>R</i> (Å)	σ^2 (Å ²)	<i>N</i>	<i>R</i> (Å)	σ^2 (Å ²)	<i>N</i>	<i>R</i> (Å)	σ^2 (Å ²)	
U-O _{yl}	2 ^a	1.776	0.001	2 ^a	1.784	0.002	2 ^a	1.788	0.002	2 ^a	1.775	0.001	
U-O _{eq}	6 ^a	2.472	0.007	6 ^a	2.489	0.008	6 ^a	2.485	0.010	6 ^a	2.470	0.007	
U-S	3 ^a	3.136	0.003	3 ^a	3.158	0.004	3 ^a	3.157	0.005	3 ^a	3.145	0.004	
S_0^2		0.737 ± 0.062			0.783 ± 0.058			0.758 ± 0.066			0.723 ± 0.057		
ΔE_0 (eV)		4.576 ± 0.698			6.075 ± 0.841			6.262 ± 1.118			4.606 ± 0.948		
<i>R</i> -factor		0.039			0.042			0.060			0.048		
<i>ss</i> -yl		0.00093 ± 0.00053			0.00224 ± 0.00055			0.00170 ± 0.00059			0.00119 ± 0.00053		
<i>N</i> _{bi}		3 ^a			3 ^a			3 ^a			3 ^a		
<i>ss</i> -obi		0.00729 ± 0.00109			0.00836 ± 0.00112			0.00959 ± 0.00172			0.00741 ± 0.00098		
<i>ss</i> -sbi		0.00288 ± 0.00055			0.00432 ± 0.00071			0.00520 ± 0.00102			0.00367 ± 0.00076		

Good fits are obtained for all the x[TOAH]₂[SO₄] ratios, confirming the structure with three bidentate sulphates. As expected from the qualitative study of the data, the U-O_{yl}, U-O_{eq}, and U-S bond lengths do not vary. However, although this does not lead to outliers, the quality of the fit deteriorates for the higher x[TOAH]₂[SO₄] ratios: the *R*-factor increases from 3.9% to 6.0% (see Figure 6a). Furthermore, as shown in Figure 6b, the Debye–Waller factor increases, suggesting more disorder in the complexes. The evolution of these two parameters indicates that the U–3 sulphate complex is destabilized, which could explain the loss in uranium extraction for high x[TOAH]₂[SO₄] ratios.

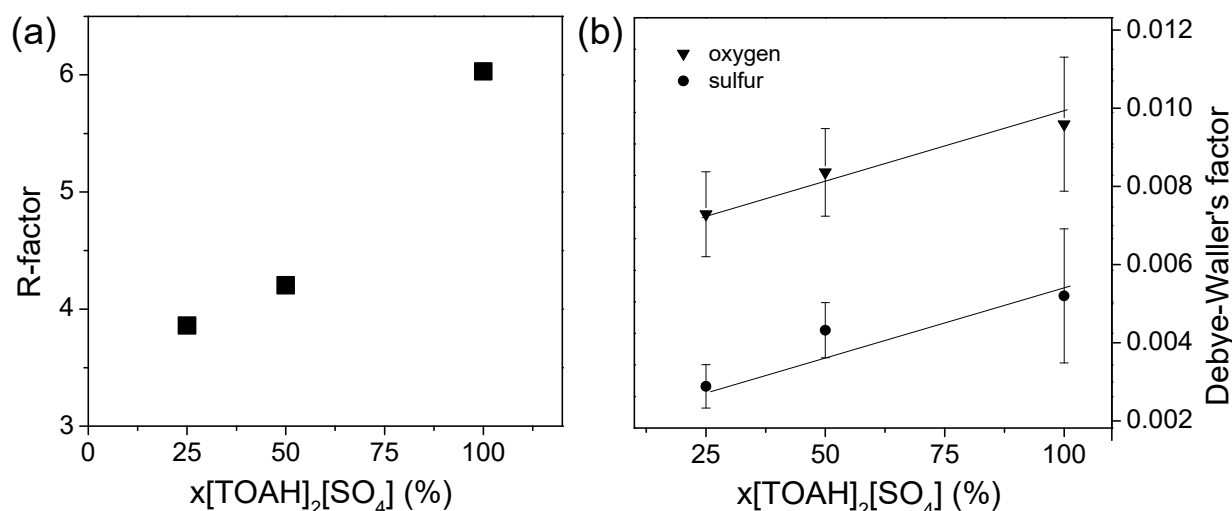


Figure 6. Evolution of (a) *R*-factor and (b) Debye–Waller factor accounting for disorder.

In conclusion, the ¹⁹F-NMR, UV-vis, and EXAFS data indicate that there are no mixed complexes formed with sulphates and NTf₂ in the first coordination sphere. However, the destabilization of the bidentate sulphate complex is observed when the x[TOAH]₂[SO₄] ratio reaches 100%, which may be related to the decrease in uranium extraction observed for these high ratios.

As extracted water is very important at these ratios, it would have been interesting to evaluate its contribution to the complexes. However, it was not possible to include it distinctly in the fits as the signatures of the monodentate U-SO_4 and $\text{U-H}_2\text{O}$ bonds are too similar (same distance, same properties). EXAFS therefore does not allow us to conclude if water competes or not with the uranium sulphate.

3.2.3. FT-IR Spectroscopy: Looking at the Second Coordination Sphere and Beyond

The Fourier transform infrared (FT-IR) spectra of protonated tertiary amine mixtures are presented in Figure 7, Figures S2 and S3. Three main bands can be distinguished in the region $800\text{--}1000\text{ cm}^{-1}$. The identification of resonance bands has been performed according to the results proposed in the literature based on a IR study dedicated to the structure of the tridecylammonium sulphate in the presence of uranium [36]. The three bands were therefore assigned to monodentate water-bound sulphates $\nu(\text{S-OH})$ at 855 cm^{-1} , to the uranyl motif $\nu(\text{UO}_2^{2+})$ at 914 cm^{-1} , and to bidentate uranium-bound sulphates $\nu(\text{S-(O...U)})_2$ at 967 cm^{-1} .

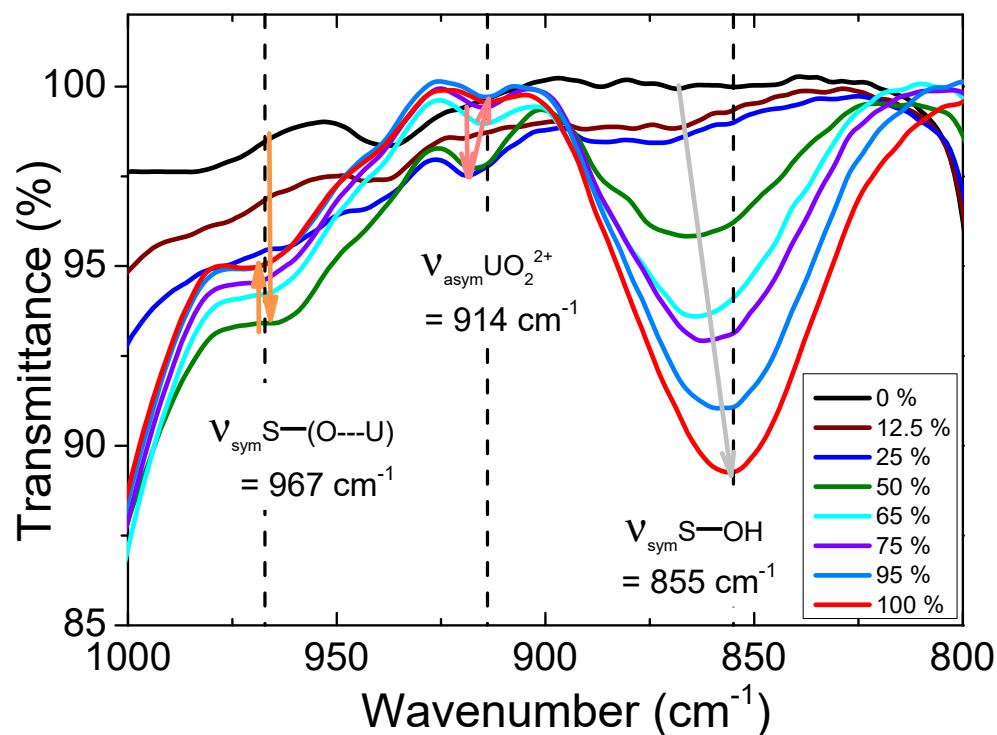


Figure 7. FT-IR spectra between 800 and 1000 cm^{-1} of the mixtures $[\text{TOAH}]_2[\text{SO}_4] + [\text{TOAH}][\text{NTf}_2]$ after contact with an aqueous phase containing $2500\text{ mg}\cdot\text{L}^{-1}$ U(VI) , $0.1\text{ mol}\cdot\text{L}^{-1}$ sulfuric acid, and $1\text{ mol}\cdot\text{L}^{-1}$ ammonium sulphate. $\text{A/O} = 4$.

A linear shift of the $\nu(\text{S-OH})$ absorption band towards the lower frequencies can be observed with the increasing molar ratio of sulphate. It indicates that sulphate becomes increasingly free (see Figure S4). The area under these $\nu(\text{S-OH})$ band curves is plotted in Figure 8a. It shows an increase after the ratio $x[\text{TOAH}]_2[\text{SO}_4] = 30\%$ that follows the trend of the water extraction profile (see Figure 3b). This first observation suggests that the sulphates are not only involved in the uranyl complexes but also more and more connected with water, whose concentration is significantly increasing at high $x[\text{TOAH}]_2[\text{SO}_4]$ ratios.

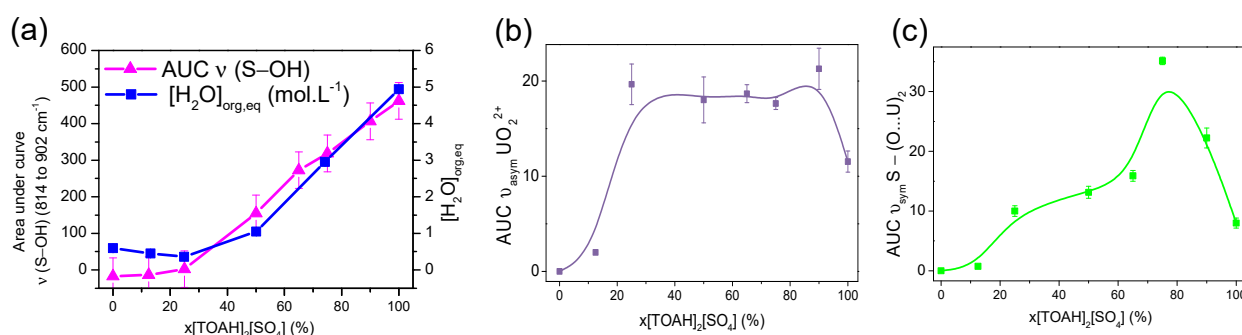


Figure 8. Integration of the characteristic bands of (a) $\nu(\text{S-OH})$, (b) $\nu(\text{UO}_2^{2+})$, and (c) $\nu(\text{S-(O..U)}_2)$ as a function of $x[\text{TOAH}]_2[\text{SO}_4]$.

To highlight the bands related to uranium, it was necessary to subtract the signal of the pre-contacted samples. After the subtraction, each band of interest was fitted with a Voigt function. The area under the curve (AUC) is plotted in Figure 8b,c as a function of $x[\text{TOAH}]_2[\text{SO}_4]$ for the $\nu(\text{UO}_2^{2+})$ and $\nu(\text{S-(O..U)}_2)$ bands.

It is interesting to note that the area under the bands attributed to the $\nu(\text{UO}_2^{2+})$ and $\nu(\text{S-(O..U)}_2)$ bands follows a similar trend to that of the uranium extraction profile (plotted in Figure 2a); it is initially constant up to $x[\text{TOAH}]_2[\text{SO}_4] = 12.5\%$, then intensifies up to $x[\text{TOAH}]_2[\text{SO}_4] = 75\%$, and decreases thereafter.

This infrared study indicates, therefore, that for $x[\text{TOAH}]_2[\text{SO}_4]$ ratios above 75%, the uranium–sulphate bond is less present to the benefit of the sulphate–water bond, suggesting a competition between the sulphate–uranium and sulphate–water complexes.

To interpret the overall uranium extraction profile of the $[\text{TOAH}]_2[\text{SO}_4] + [\text{TOAH}][\text{NTf}_2]$ mixture (Figure 2a), it is necessary to take into account all the data obtained by the spectroscopic methods, as well as the water extraction data and the acid release from the organic to the aqueous phase (Figure 3b,c). The spectroscopic data indicate that the NTf_2^- anion is not involved in the extraction of uranium. As in the conventional medium (TOA + dodecane), uranium is extracted by the TOAH^+ protonated amines and three bidentate sulphates in the first coordination sphere.

For low $x[\text{TOAH}]_2[\text{SO}_4]$ ratios of 0–25%, uranium extraction does not increase, while the amount of sulphates introduced into the organic phase does. This effect can be explained by the increased release of H^+ protons from the organic phase into the aqueous phase. This release reduces the number of protonated amines available, inhibiting uranium extraction.

From $x[\text{TOAH}]_2[\text{SO}_4] = 25\%$, the proton release stabilizes and then decreases, leading to an increase in the number of TOAH^+ protonated amines available. This increase in TOAH^+ , accompanied by an increase in sulphates with $x[\text{TOAH}]_2[\text{SO}_4]$, is therefore consistent with the very sharp increase in uranium extraction between $x[\text{TOAH}]_2[\text{SO}_4] = 25$ and 75%.

Beyond this ratio, the very sharp increase in extracted water leads, as previously suggested, to a competition between the sulphate–uranium and sulphate–water complexes, which destabilizes the uranyl trisulphate complexes and leads to saturation and then to a decrease in uranium extraction.

This study shows that the main elements responsible for uranium extraction are sulphates and protonated amines and that the availability of the latter is regulated by the concentration of extracted water, as well as by the release of acidic protons from the organic phase to the aqueous phase.

A deeper understanding of these phenomena would require an interpretation of the nonlinear behavior of the water extraction and the origin of the H^+ proton release. The increased extraction of water can be partially explained by the difference in hydrophilicity between NTf_2^- and SO_4^{2-} anions, but its nonlinear extraction might be related to the activity of the aqueous phase and to the chemical potential equilibria between the species present in the aqueous and organic phases. The chemical potential equilibrium may also be

responsible for the release of protons from the organic phase to the aqueous phase. These equilibria are, however, very difficult to pin down and predict.

4. Conclusions

Several organic extractants based on protonated tertiary amines or quaternary ammoniums and their mixtures were evaluated for the extraction of uranium under the AMEX process conditions. Irrespective of the leachate and the cation used, nonlinearities in the uranium extraction were observed as a function of the sulphate ratio in the organic phase. This effect, which allows a very high extraction efficiency for some mixtures to be obtained, can be advantageously considered for optimized uranium extraction or when the physico-chemical properties (such as viscosity or density) of the final solvent need to be adjusted. The origins of these nonlinearities were therefore investigated with a mechanistic study.

An extensive analysis of the amounts of extracted water, acid, and uranium, combined with detailed spectroscopic studies (NMR, UV-vis, FT-IR, and EXAFS) of the contacted organic phases, was carried out on the $[\text{TOAH}]_2[\text{SO}_4] + [\text{TOAH}][\text{NTf}_2]$ system to understand the three regimes of extraction observed, along with the sulphate ratios. Whatever the $x[\text{TOAH}]_2[\text{SO}_4]$ ratio, the NTf_2^- anion was shown to be absent in the first coordination sphere. It was shown that uranium extraction takes place via four protonated amines and three bidentate sulphates, as in the conventional AMEX process. An analysis of EXAFS data showed, moreover, that the bidentate uranium–sulphate complex is destabilized for high $x[\text{TOAH}]_2[\text{SO}_4]$ ratios. The infrared spectroscopy revealed that, along with this destabilization, the number of sulphate–uranium bonds decreased in favor of sulphate–water bonds. It is assumed that a competition between sulphate–water and sulphate–uranyl complexes governs the extraction loss observed at high $x[\text{TOAH}]_2[\text{SO}_4]$ ratios.

To understand the observed nonlinearities over the whole range of $x[\text{TOAH}]_2[\text{SO}_4]$ ratios, the release of acid from the organic phase into the aqueous phase as well as the non-linear water extraction were further considered. The nonlinear extraction of uranium was finally related to the concentration of protonated amines and sulphates: (i) by influencing the number of available protonated amines in the organic phase, as acid release negatively affects uranium extraction at low $x[\text{TOAH}]_2[\text{SO}_4]$ ratios; (ii) in the medium $x[\text{TOAH}]_2[\text{SO}_4]$ ratios, the saturation of acid release induces a strong increase in the available protonated amines, leading to a strong increase in uranium extraction; (iii) at higher $x[\text{TOAH}]_2[\text{SO}_4]$ ratios, the strong increase in water extraction destabilizes the uranyl–sulphate complexes because of a competition between sulphate–water and sulphates–uranyl complexes.

Water extraction is therefore one of the main parameters governing the extraction mechanisms of such systems. As it was already observed in different ionic liquid systems, it is also likely to govern physicochemical properties such as density and viscosity. Finding an optimized mixture of ionic liquids for solvent extraction requires, therefore, an elucidation of the water extraction properties of the systems.

Supplementary Materials: The following supporting information can be downloaded at: <https://www.mdpi.com/article/10.3390/separations10090509/s1>, ESI 1: Synthesis of protonated tertiary amines and quaternary ammoniums, Figure S1: Water content of $[\text{TOAH}]_2[\text{SO}_4] + [\text{TOAH}][\text{NTf}_2]$ as a function of $x[\text{TOAH}]_2[\text{SO}_4]$, Figure S2: FT-IR spectra of different $x[\text{TOAH}]_2[\text{SO}_4]$ ratios, Figure S3: Infra-red spectra of $x[\text{TOAH}]_2[\text{SO}_4] = 65\%$ mixture before contact (dry) and after contact, Figure S4: Illustration of linear shift towards the lower frequencies.

Author Contributions: E.G.: investigation, data curation, writing—original draft. S.D.: writing, review. Z.L.: investigation, data curation. T.D.: EXAFS spectroscopy measurements and analysis. G.A.: NMR spectroscopy measurements, review. F.G.: review. P.-L.S.: local contact for EXAFS spectroscopy. S.P.-R.: project administration, resources, supervision, funding acquisition. All authors have read and agreed to the published version of the manuscript.

Funding: We acknowledge the NEEDS program as well as CEA for their funding.

Data Availability Statement: Data will be made available on request.

Acknowledgments: We acknowledge SOLEIL and beamline MARS for the provision of the synchrotron radiation facilities and assistance. We also thank Beatrice Baus-Lagarde for her help with the ICP-OES measurements and David Lemire for his participation in the EXAFS experiment.

Conflicts of Interest: The authors declare that they have no known competing financial interests or personal relationships that could have appeared to influence the work reported in this paper.

References

1. Crouse, D.J.; Brown, K.B. The Amex Process for Extracting Thorium Ores with Alkyl Amines. *Ind. Eng. Chem.* **1959**, *51*, 1461–1464. [[CrossRef](#)]
2. Sato, T.; Watanabe, H.; Suzuki, H. Liquid-Liquid Extraction of Molybdenum(VI) from Aqueous Acid Solutions by High-Molecular Weight Amines. *Solvent Extr. Ion Exch.* **1986**, *4*, 987–998. [[CrossRef](#)]
3. Sato, T.; Watanabe, H. The Extraction of Zirconium(IV) from Sulfuric Acid Solutions by Long-Chain Alkyl Quaternary Ammonium Compound. *Sep. Sci. Technol.* **1982**, *17*, 625–634. [[CrossRef](#)]
4. Chagnes, A.; Fosse, C.; Courtaud, B.; Thiry, J.; Cote, G. Chemical Degradation of Trioctylamine and 1-Tridecanol Phase Modifier in Acidic Sulfate Media in the Presence of Vanadium (V). *Hydrometallurgy* **2011**, *105*, 328–333. [[CrossRef](#)]
5. Solgy, M.; Taghizadeh, M.; Ghodocynejad, D. Adsorption of Uranium(VI) from Sulphate Solutions Using Amberlite IRA-402 Resin: Equilibrium, Kinetics and Thermodynamics Study. *Ann. Nucl. Energy* **2015**, *75*, 132–138. [[CrossRef](#)]
6. Kumar, P.; Pal, A.; Saxena, M.K.; Ramakumar, K.L. Supercritical Fluid Extraction of Uranium and Thorium from Solid Matrices. *Desalination* **2008**, *232*, 71–79. [[CrossRef](#)]
7. Smolinski, T.; Wawszczak, D.; Deptula, A.; Lada, W.; Olczak, T.; Rogowski, M.; Pyszynska, M.; Chmielewski, A.G. Solvent Extraction of Cu, Mo, V, and U from Leach Solutions of Copper Ore and Flotation Tailings. *J. Radioanal. Nucl. Chem.* **2017**, *314*, 69–75. [[CrossRef](#)]
8. Quijada-Maldonado, E.; Olea, F.; Sepúlveda, R.; Castillo, J.; Cabezas, R.; Merlet, G.; Romero, J. Possibilities and Challenges for Ionic Liquids in Hydrometallurgy. *Sep. Purif. Technol.* **2020**, *251*, 117289. [[CrossRef](#)]
9. Yan, Q.; Cai, Y.; Wang, Z.; Dong, X.; Yuan, L.; Feng, W.; Chen, J.; Xu, C. Separation of Americium from Lanthanide by a Task-Specific Ionic Liquid Decorated with 2,6-Bis-Triazolyl-Pyridine Moiety. *Sep. Purif. Technol.* **2022**, *299*, 121752. [[CrossRef](#)]
10. Brown, K.B.; Coleman, C.F.; Crouse, D.J.; Denis, J.O.; Moore, J.G. *The Use of Amines as Extractants for Uranium from Acidic Sulfate Liquors. A Preliminary Report*; United States Atomic Energy Commission: Germantown, MD, USA, 1954; pp. 1–122. [[CrossRef](#)]
11. Lu, Z.; Dourdain, S.; Pellet-Rostaing, S.; Arrachart, G.; Giusti, F. Mélanges de Sels d’ammonium Quaternaire Pour l’extraction de l’uranium(VI) de Solutions Aqueuses d’acide Sulfurique. Patent FR3116936 A1 WO2022117942 (A1), 3 June 2022.
12. Guerinoni, E.; Dourdain, S.; Lu, Z.; Giusti, F.; Arrachart, G.; Couturier, J.; Hartmann, D.; Pellet-Rostaing, S. Highly Efficient Diluent-Free Solvent Extraction of Uranium and Comparative Life Cycle Assessment with the Conventional Solvent. *Accept. Hydrometall.* **2023**.
13. Ghandi, K. A Review of Ionic Liquids, Their Limits and Applications. *GSC* **2014**, *4*, 44–53. [[CrossRef](#)]
14. Greaves, T.L.; Drummond, C.J. Protic Ionic Liquids: Properties and Applications. *Chem. Rev.* **2008**, *108*, 206–237. [[CrossRef](#)] [[PubMed](#)]
15. Keshapolla, D.; Srinivasarao, K.; Gardas, R.L. Influence of Temperature and Alkyl Chain Length on Physicochemical Properties of Trihexyl- and Trioctylammonium Based Protic Ionic Liquids. *J. Chem. Thermodyn.* **2019**, *133*, 170–180. [[CrossRef](#)]
16. Billard, I.; Ouadi, A.; Gaillard, C. Is a Universal Model to Describe Liquid-Liquid Extraction of Cations by Use of Ionic Liquids in Reach? *Dalton Trans.* **2013**, *42*, 6203–6212. [[CrossRef](#)] [[PubMed](#)]
17. Dukov, I.L.; Atanassova, M. Effect of the Diluents on the Synergistic Solvent Extraction of Some Lanthanides with Thenoyltrifluoroacetone and Quaternary Ammonium Salt. *Hydrometallurgy* **2003**, *68*, 89–96. [[CrossRef](#)]
18. Dietz, M.L.; Dzielawa, J.A.; Laszak, I.; Young, B.A.; Jensen, M.P. Influence of Solvent Structural Variations on the Mechanism of Facilitated Ion Transfer into Room-Temperature Ionic Liquids. *Green Chem.* **2003**, *5*, 682–685. [[CrossRef](#)]
19. Billard, I.; Ouadi, A.; Jobin, E.; Champion, J.; Gaillard, C.; Georg, S. Understanding the Extraction Mechanism in Ionic Liquids: $\text{UO}_2^{2+}/\text{HNO}_3/\text{TBP}/\text{C}_4\text{-MimTf N}$ as a Case Study. *Solvent Extr. Ion Exch.* **2011**, *29*, 577–601. [[CrossRef](#)]
20. Wionczyk, B.; Apostoluk, W. Solvent Extraction of Chromium(III) from Alkaline Media with Quaternary Ammonium Compounds. Part I. *Hydrometallurgy* **2004**, *72*, 185–193. [[CrossRef](#)]
21. Rout, A.; Venkatesan, K.A.; Srinivasan, T.G.; Vasudeva Rao, P.R. Ionic Liquid Extractants in Molecular Diluents: Extraction Behavior of Europium (III) in Quaternary Ammonium-Based Ionic Liquids. *Sep. Purif. Technol.* **2012**, *95*, 26–31. [[CrossRef](#)]
22. Jaree, A.; Khunphakdee, N. Separation of Concentrated Platinum(IV) and Rhodium(III) in Acidic Chloride Solution via Liquid-Liquid Extraction Using Tri-Octylamine. *J. Ind. Eng. Chem.* **2011**, *17*, 243–247. [[CrossRef](#)]
23. Biswas, S.; Basu, S. Extraction of Zirconium(IV) from Hydrochloric Acid Solutions by Tri-Octylamine and Neutral Donors. *J. Radioanal. Nucl. Chem.* **2006**, *242*, 253–258. [[CrossRef](#)]
24. Wang, Y.; Liu, X.; Yang, A.; Lv, P.; Zhang, L.; Li, Y.; Yang, Y. Extraction and Separation on Au(III) and Pt(IV) from HCl Media Using Novel Piperazine-Based Ionic Liquid as an Ionic Exchanger. *J. Mol. Liq.* **2022**, *353*, 118846. [[CrossRef](#)]
25. Xue, W.; Liu, R.; Liu, X.; Wang, Y.; Lv, P.; Yang, Y. Selective Extraction of Nd(III) by Novel Carboxylic Acid Based Ionic Liquids without Diluent from Waste NdFeB Magnets. *J. Mol. Liq.* **2022**, *364*, 119919. [[CrossRef](#)]

26. Hu, Q.; Zhao, J.; Wang, F.; Huo, F.; Liu, H. Selective Extraction of Vanadium from Chromium by Pure [C₈mim][PF₆]: An Anion Exchange Process. *Sep. Purif. Technol.* **2014**, *131*, 94–101. [[CrossRef](#)]
27. Zuo, Y.; Liu, Y.; Chen, J.; Li, D.Q. The Separation of Cerium(IV) from Nitric Acid Solutions Containing Thorium(IV) and Lanthanides(III) Using Pure [C₈mim]PF₆ as Extracting Phase. *Ind. Eng. Chem. Res.* **2008**, *47*, 2349–2355. [[CrossRef](#)]
28. Ouadi, A.; Klimchuk, O.; Gaillard, C.; Billard, I. Solvent Extraction of U(VI) by Task Specific Ionic Liquids Bearing Phosphoryl Groups. *Green Chem.* **2007**, *9*, 1160–1162. [[CrossRef](#)]
29. Rout, A.; Binnemans, K. Solvent Extraction of Neodymium(III) by Functionalized Ionic Liquid Trioctylmethylammonium Dioctyl Diglycolamate in Fluorine-Free Ionic Liquid Diluent. *Ind. Eng. Chem. Res.* **2014**, *53*, 6500–6508. [[CrossRef](#)]
30. Sukhbaatar, T.; Duvail, M.; Dumas, T.; Dourdain, S.; Arrachart, G.; Solari, P.L.; Guilbaud, P.; Pellet-Rostaing, S. Probing the Existence of Uranyl Trisulfate Structures in the AMEX Solvent Extraction Process. *Chem. Commun.* **2019**, *55*, 7583–7586. [[CrossRef](#)]
31. Marták, J.; Schlosser, Š. Density, Viscosity, and Structure of Equilibrium Solvent Phases in Butyric Acid Extraction by Phosphonium Ionic Liquid. *J. Chem. Eng. Data* **2017**, *62*, 3025–3035. [[CrossRef](#)]
32. Hanke, K.; Kaufmann, M.; Schwaab, G.; Havenith, M.; Wolke, C.T.; Gorlova, O.; Johnson, M.A.; Kar, B.P.; Sander, W.; Sanchez-Garcia, E. Understanding the Ionic Liquid [NC₄₁₁₁][NTf₂] from Individual Building Blocks: An IR-Spectroscopic Study. *Phys. Chem. Chem. Phys.* **2015**, *17*, 8518–8529. [[CrossRef](#)]
33. Servaes, K.; Hennig, C.; Billard, I.; Gaillard, C.; Binnemans, K.; Görller-Walrand, C.; Van Deun, R. Speciation of Uranyl Nitrate Complexes in Acetonitrile and in the Ionic Liquid 1-Butyl-3-Methylimidazolium Bis(Trifluoromethylsulfonyl)Imide. *Eur. J. Inorg. Chem.* **2007**, *2007*, 5120–5126. [[CrossRef](#)]
34. Görller-Walrand, C.; Jaegere, S.D. Étude comparative des spectres d'absorption de complexes d'uranyle en solution et à l'état solide. Complexes de symétrie Cs, D_{2h} (6) ET D_{3h} (6). *J. Chim. Phys.* **1972**, *69*, 726–736. [[CrossRef](#)]
35. Hennig, C.; Kraus, W.; Emmerling, F.; Ikeda, A.; Scheinost, A.C. Coordination of a Uranium(IV) Sulfate Monomer in an Aqueous Solution and in the Solid State. *Inorg. Chem.* **2008**, *47*, 1634–1638. [[CrossRef](#)] [[PubMed](#)]
36. Lipovskii, A.A.; Kuzina, M.G. The Infrared Absorption Spectra and Structure of Tridecylammonium Sulphate, Tridecylammonium Hydrogensulphate, and Tridecylammonium Dioxotrisulphatouranate (VI). *Russ. J. Inorg. Chem.* **1965**, *10*, 740–745.

Disclaimer/Publisher's Note: The statements, opinions and data contained in all publications are solely those of the individual author(s) and contributor(s) and not of MDPI and/or the editor(s). MDPI and/or the editor(s) disclaim responsibility for any injury to people or property resulting from any ideas, methods, instructions or products referred to in the content.